

Coupling of Vibrational Excitation to the Rotational Motion of a Single Adsorbed Molecule

B. C. Stipe, M. A. Rezaei, and W. Ho

Laboratory of Atomic and Solid State Physics and Center for Materials Research, Cornell University, Ithaca, New York 14853

(Received 16 March 1998)

The reversible rotation of a single isolated acetylene molecule between two diagonal sites on the Cu(100) surface at 8 K was induced and monitored with tunneling electrons from a scanning tunneling microscope (STM). Excitation of the C—H (C—D) stretch mode of C_2H_2 (C_2D_2) at 358 meV (266 meV) led to a 10-fold (60-fold) increase in the rotation rate. This increase is attributed to energy transfer from the C—H (C—D) stretch mode to the hindered rotational motion of the molecule. Inelastic electron tunneling spectroscopy with the STM provides the energies of the stretch modes and allows a quantitative determination of the inelastic tunneling and coupling probabilities. [S0031-9007(98)06800-8]

PACS numbers: 68.35.Ja, 07.79.Cz, 34.50.Ez, 61.16.Ch

The concept of the reaction coordinate hinges on the notion that motions of specific bonds dictate the progress of the reaction. By selectively exciting these bonds, the rates and pathways of chemical reactions can be affected. In addition to selective deposition of energy into the reaction coordinates, it is necessary for the reaction to occur prior to the dissipation and randomization of the initially localized energy [1–4]. Fast energy transfer has been the bottleneck in the realization of bond-selected chemistry.

The unique capabilities of the scanning tunneling microscope (STM) allow one to excite individual molecules and observe the resulting motions. For example, it was demonstrated that tunneling electrons from the STM can be used to induce and image the dissociation of an isolated O_2 molecule adsorbed on the Pt(111) surface [5]. Inelastic tunneling electrons were used to excite the reaction coordinate, the $\nu(OO)$ stretch. Excitation of the hindered rotational mode of the nearly parallel bonded O_2 molecule also led to its reversible rotation [6]. By scanning the STM tip at a high bias voltage, reversible rotation of antimony dimers on the Si(100) surface was also observed [7]. Using a tracking technique, quantitative studies were made on the reversible rotation rates of individual Si ad-dimers on the Si(100) surface as a function of temperature and electric field [8].

In this paper, tunneling electrons were used to induce and monitor the motions of a single molecule, namely, acetylene adsorbed on Cu(100) at 8 K. We demonstrate a novel application of the STM to directly probe the coupling of a specific vibrational mode of the molecule to its hindered rotational motion. Even though intramolecular energy transfer has been investigated extensively in the gas phase by lasers [1,2], the STM allows a direct and clear visualization of the process. Single molecule vibrational spectroscopy allows the deduction of this coupling and a quantitative determination of the coupling probability. The induced rotation rate was found to decrease as the STM tip was laterally displaced away from the center of the molecule and exhibited an anisotropic spatial dependence of molecular dimensions. It is shown how the

analysis of single-molecule vibrational modes and single-molecule motions can enhance our understanding of energy transfer at atomic length scales.

The STM is homemade and operates in ultrahigh vacuum [9]. The temperature of both the sample and the STM can be varied over the range 8 to 350 K. The polycrystalline tungsten tip was prepared by sputtering and annealing. Large defect-free regions of the Cu(100) surface were obtained with repeated cycles of 1 keV Ne^+ sputtering and annealing at 500 °C. The sample was dosed *in situ* with acetylene until a coverage of about 0.001 monolayer was observed in STM images. Throughout the entire experiment, the sample temperature was maintained at 8 K with a stability of better than 0.01 K. The STM tip was precisely positioned over a molecule of interest by tracking a local extremum in the STM topographical image with the feedback on and applying a known offset parallel to the surface. To induce the rotation of the molecule, the feedback was then turned off, a voltage pulse was applied to the sample, and the tunneling current was recorded during the pulse. Only isolated molecules were studied quantitatively since neighboring adsorbates can have a dramatic influence on the rotational motion [6].

An x-ray absorption study concluded that the C—C bond of acetylene is parallel to the surface and significantly lengthened [10]. Rehybridization leads to a bent geometry [11] as depicted in Fig. 1a. The STM images are consistent with the plane of the molecule perpendicular to the surface and across the diagonal of the square formed by four Cu atoms. The “dumbbell” shape is attributed to π bonding to the Cu atoms perpendicular to the C—C axis.

After positioning the tip and increasing the sample bias voltage, sudden changes in the tunneling current are recorded as the molecule undergoes reversible rotation between the two equivalent orientations (Fig. 1b). A bistable current is observed with the high (low) value corresponding to the orientation with the tip inside (outside) the plane of the molecule. Plots of the time intervals spent

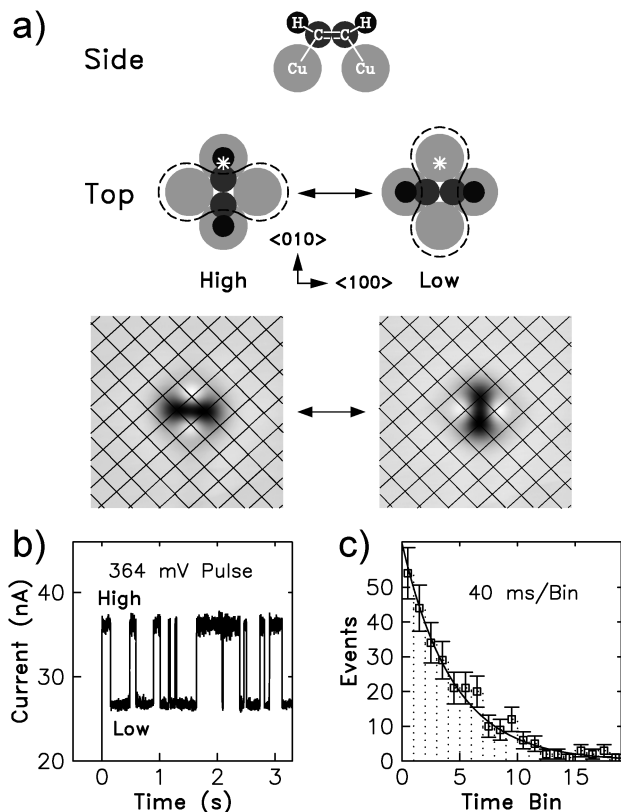


FIG. 1. (a) Schematic drawing of acetylene on the Cu(100) surface showing side and top views of the molecular adsorption site and orientations consistent with the STM images. The dashed line represents the outline of the dumbbell shaped depression in STM images. The asterisk shows the off-center position of the tip over the molecule. In the corresponding STM images, the square lattice represents the Cu atoms of the substrate and was taken from an atomic resolution image of the same area with the C_2H_2 molecule adsorbed on the tip. The distance between Cu atoms is 2.55 Å. The images were scanned at a tunneling current of 10 nA and a sample bias of 100 mV. (b) Current during a 364 mV voltage pulse over a C_2H_2 molecule initially in the high current orientation; tip remains fixed 1.5 Å off center. Each jump in the current indicates the moment of rotation of the molecule. (c) Distribution of the times the molecule spent in the high-current orientation with a fit to an exponential decay. The fitted time constant is 184 ms. The analysis includes a total of 278 time intervals.

in the two orientations exhibit the expected exponential distributions (results for the high-current level are shown in Fig. 1c). The inverse of the time constant of this exponential decay gives the rate of rotation for the chosen sample bias voltage and current. Results shown in this paper are for positive sample bias voltage. At negative bias, rates of rotation were reduced by approximately a factor of 2.

The rotation rates depend strongly on the injection point of the tunneling current as given by the position of the tip. The rates show a monotonic decrease as the tip is moved away from the center of the molecule both inside (Fig. 2a) and outside (Fig. 2b) the plane of the molecule.

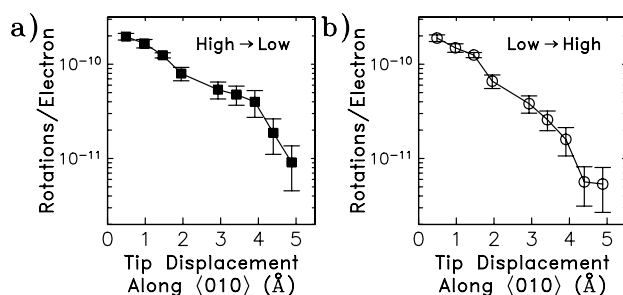


FIG. 2. C_2H_2 rotation rates normalized to the current are shown as a function of tip displacement from the center of the molecule along the $\langle 010 \rangle$ direction (see Fig. 1a). (a) Rotations per electron from the high current orientation to the low-current orientation. (b) Rotations per electron from the low-current orientation to the high-current orientation. Data taken for a sample bias voltage of 400 mV and a tunneling current of approximately 4 nA.

The dropoff in the rotation rate is anisotropic; rates decrease faster for the low-current orientation than for the high-current orientation. The effective range of rotation corresponds to the spatial extent of the molecule in the STM image. Such a spatial dependence suggests orbital specificity in the coupling of the tunneling electrons to the rotation of the molecule.

A linear dependence of the rotation rate as a function of the tunneling current is found for both C_2H_2 and C_2D_2 at various bias voltages below 10 nA. When the rotation rate is normalized to the tunneling rate, a constant is obtained (Fig. 3a). Similar results are obtained for tip positions both inside and outside the plane of the molecule. The linear dependence of the rotation rate on tunneling current indicates a rotation mechanism involving the inelastic tunneling of a single electron. Deviations from linearity can be seen for currents higher than 10 nA suggesting the increasing importance of excitation by more than

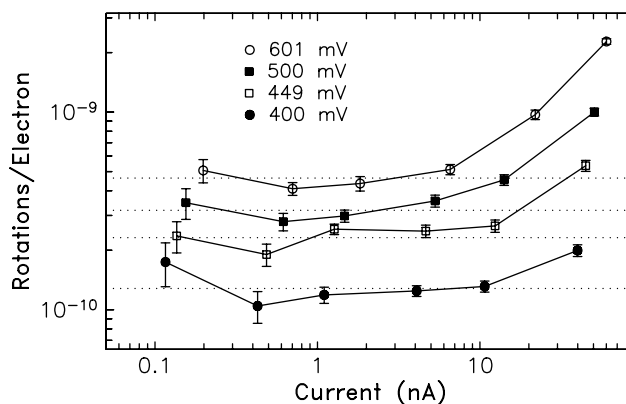


FIG. 3. C_2H_2 rotations per electron as a function of tunneling current for various sample bias voltages. The tip was positioned 1.5 Å laterally from the center of the molecule in the $\langle 010 \rangle$ direction. Data shown are for rotation from the high-current orientation to the low-current orientation. Dotted lines are least-squares fits to a constant using the first four data points at each voltage.

one electron. Only when the tunneling rate is less than the vibrational relaxation rate, would one theoretically expect a single electron process to dominate [12]. This is consistent with the crossover from single to multiple electron processes observed here.

The dependence of the rotation rate on the sample bias voltage at a chosen tunneling current shows a 10-fold increase near 358 mV for C_2H_2 and a 60-fold increase near 266 mV for C_2D_2 (Fig. 4a). By tuning the energy of the tunneling electrons, the rotation rate for C_2D_2 was as much as 40 times higher than for C_2H_2 under the same tunneling conditions. Derivatives of the data show the narrow voltage range of 20 mV over which the increases in rotation rates occur (Fig. 4b). These voltages correspond to the peak positions observed in single molecule inelastic electron tunneling spectroscopy with the STM (STM-IETS) [13]. The 358 mV peak in d^2I/dV^2 results from the excitation of the C—H stretch mode of C_2H_2 , which shows the expected isotopic shift to 266 mV for

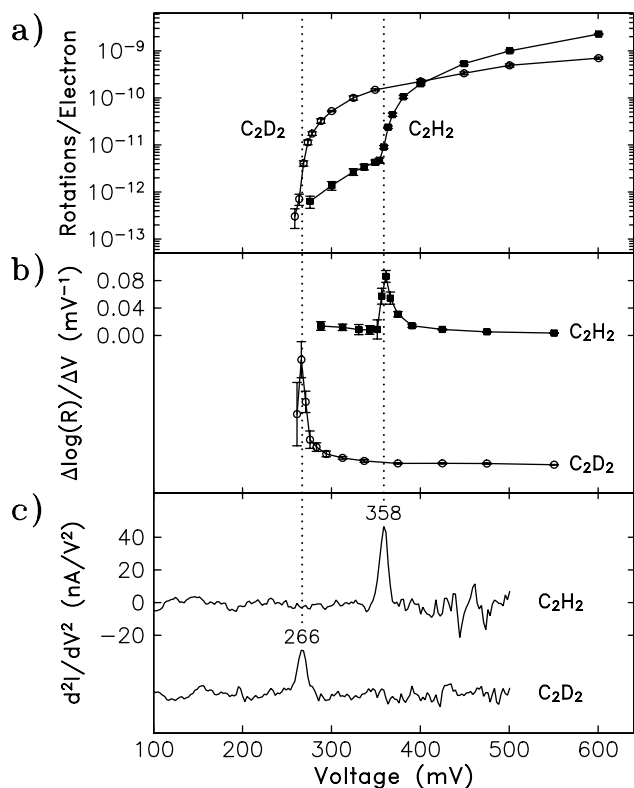


FIG. 4. (a) Rotations per electron for both C_2H_2 and C_2D_2 as a function of sample bias voltage. Tunneling current used was approximately 40 nA. Otherwise, the experimental conditions were the same as in Fig. 3. (b) The slopes of the data in (a). (c) d^2I/dV^2 spectra for C_2H_2 and C_2D_2 show STM-IETS vibrational peaks at 358 mV and 266 mV, respectively. The tip was the same one used to collect the rotation data. The increase in noise above the peak for C_2H_2 is the result of the rotation of the molecule and a very slightly off-center tip position (within 0.2 Å of center). The tip was fixed in position vertically to give a dc tunneling current of 1 nA at 249 mV sample bias. A rms modulation voltage of 5 mV was used. The spectrum is an average over four voltage ramps of 2 min each.

the C—D stretch mode of C_2D_2 (Fig. 4c). The change in tunneling conductance, $\sigma = dI/dV$, across the peaks shown due to the inelastic tunneling channel is $\Delta\sigma/\sigma = 11.8 \pm 0.2\%$ and $8.6 \pm 0.2\%$ for C_2H_2 and C_2D_2 , respectively. Such large inelastic tunneling conductances are more consistent with a resonant tunneling mechanism than the dipole scattering mechanism [13,14]. These results clearly demonstrate that the dominant pathway for rotation is via the intermediate excitation of the C—H or C—D stretch when these excitations are energetically allowed.

All results presented here were obtained with the same tip. When a second, slightly blunter tip was used to repeat the experiments, the rotation rates were found to fall off less quickly with lateral tip displacement (the dependence on current and voltage did not change). Compared to the results presented in Fig. 2, the rotation rate was $40 \pm 10\%$ lower 0.5 Å from the center of the molecule and about a factor of 2 higher 5 Å away from the molecule's center. The spatial dimensions from topographical images were also seen to broaden with the blunter tip. Furthermore, the change in the rotation rate near the center of the molecule corresponded with the change in $\Delta\sigma/\sigma$ measured by STM-IETS at the center of the molecule (the rotation rate could not be measured exactly at the center of the molecule since the tunneling currents are the same for both orientations in this case). The second tip used gave changes in tunneling conductance of $\Delta\sigma/\sigma = 6.2 \pm 0.2\%$ and $4.5 \pm 0.2\%$ for C_2H_2 and C_2D_2 , respectively—a $48 \pm 2\%$ average reduction from the sharper tip.

The changes in tunneling conductance measured by STM-IETS can provide a direct measurement of the fraction of electrons which tunnel inelastically and excite the C—H (C—D) stretch [14]. We can assume that the inelastic tunneling current increases linearly for small increments above the C—H (C—D) stretch energy. For the sharp tip used here we can use the value of $\Delta\sigma/\sigma$ above to approximate that 1% of the tunneling electrons excite the C—H stretch at 400 mV. Therefore, for each C—H excitation, the probability of rotation in the single-electron regime (<10 nA) is approximately 2×10^{-8} (see Fig. 2). A similar analysis of the C_2D_2 data in the single-electron regime yields a value of 1×10^{-8} rotations per C—D stretch excitation. The correspondence between the inelastic tunneling conductance and rotation rates for different tips confirms that the probability of rotation per C—H (C—D) stretch excitation is tip independent. This probability is also found to be independent of current (in the single-electron regime) and voltage. For example, at 450 mV approximately 2% of the tunneling electrons excite the C—H stretch in C_2H_2 and the rotation rates are approximately twice as high as at 400 mV (see Fig. 3). The inelastic current is, in general, nonlinear in voltage so the inelastic fraction becomes more uncertain for higher voltages. The small couplings of the C—H and C—D stretch modes to the rotational motion show that these

modes do not efficiently rotate the molecule. Rather, the effect observed here has much to do with the large inelastic tunneling channels which excite the C—H and C—D stretch modes. Understanding the reason for the predominance of these stretch modes over other vibrational modes in the IETS spectra would be an interesting area of theoretical research. The electron-vibration coupling constant is apparently very high between the relevant ion resonance and the C—H (C—D) stretch modes [14].

Time resolved measurements have shown that an important path for the decay of the $\nu(\text{CH})$ stretch mode of liquid hydrocarbons is via the excitation of two $\delta(\text{CH})$ bending modes [15]. In inert gas matrices, the stretching vibrations of simple hydrogenated molecules have been determined to couple efficiently to nearly free rotational modes [16,17]. For CO, the rotational motion is hindered and the energy in the $\nu(\text{CO})$ stretch is transferred to the librational modes [18]. The relaxation of $\nu(\text{CH})$ stretch in CH_3S adsorbed on Ag(111) has also been attributed to the excitation of $\delta(\text{CH})$ bending modes [19]. Although the relaxation rates on semiconductor surfaces are generally smaller than on metal surfaces, the relaxation mechanism of $\nu(\text{SiH})$ stretch for H adsorbed on Si(111) involves the excitation of the $\delta(\text{SiH})$ bending modes [20]. In condensed media, the discrepancy in energies between the stretch mode and the sum of the bending modes of the molecule can be absorbed in the low energy excitations of the media.

In view of the vibrational relaxation studies of molecules in condensed media, a likely mechanism leading to the enhancement in rotation rates of acetylene on Cu(100) involves the relaxation of the $\nu(\text{CH})$ stretch vibration to the bending vibrations. The reaction coordinate is likely to be the molecule-substrate hindered rotational mode. A more complicated rotation mechanism involving conversion to an intermediate bridge site is not likely as the molecule always rotates on the same hollow site. Electron energy loss spectroscopy measurements of C_2H_2 on Cu(100) showed peaks at 357, 164, 141, 118, 78, and 52 meV. These peaks were assigned to the $\nu(\text{CH})$ stretch, $\nu(\text{CC})$ stretch, $\delta_{as}(\text{CH})$ in-plane bend or wag, $\delta_s(\text{CH})$ in-plane bend or scissor, $\gamma(\text{CH})$ out-of-plane bend or twist, and $\nu(\text{CM})$ molecule-surface stretch, respectively [21]. Thus, the $\nu(\text{CH})$ stretch mode may relax by exciting a combination of bending and hindered rotational modes, including overtones via anharmonic coupling. The relaxation of the bending modes can lead to further energy transfer to the hindered rotational mode (reaction coordinate). Rotation occurs if enough energy is transferred to the reaction coordinate from the initial relaxation of the $\nu(\text{CH})$ stretch. For tunneling energies below the $\nu(\text{CH})$ stretch, only the bending and hindered rotational modes may be excited. Since these modes are not observed in STM-IETS, these channels are weak but apparently account for the small background rotation rate (see Fig. 4). While the coupling of the stretch vibration to the rotational motion is unambiguous, the detailed

mechanism of how this occurs is not precisely determined. The observation of vibrationally induced rotation suggests that the rate of energy relaxation via excitation of substrate modes is not fast enough to completely quench the observed motions.

With the STM, it is now possible to induce and perform detailed studies of the motions of a single adsorbed molecule. Single molecule vibrational spectroscopy with the STM can provide insight into the mechanisms which lead to nuclear motions. In future work, effects due to intermolecular interactions can be introduced and studied in a controlled manner. An understanding of the vibrational and rotational motions, and their couplings, is essential for achieving control in the making and breaking of chemical bonds.

Support of this research by the National Science Foundation under Grant No. DMR-9417866 is gratefully acknowledged.

-
- [1] F. F. Crim, *J. Phys. Chem.* **100**, 12 725 (1996).
 - [2] E. W.-G. Diau, J. L. Herek, Z. H. Kim, and A. H. Zewail, *Science* **279**, 847 (1998).
 - [3] T. J. Chuang, H. Seki, and I. Hussla, *Surf. Sci.* **158**, 525 (1985).
 - [4] W. Ho, *J. Phys. Chem.* **100**, 13 050 (1996).
 - [5] B. S. Stipe, M. A. Rezaei, W. Ho, S. Gao, M. Persson, and B. I. Lundqvist, *Phys. Rev. Lett.* **78**, 4410 (1997).
 - [6] B. S. Stipe, M. A. Rezaei, and W. Ho, *Science* **279**, 1907 (1998).
 - [7] Y. W. Mo, *Science* **261**, 886 (1993).
 - [8] B. S. Swartzentruber, A. P. Smith, and H. Jonsson, *Phys. Rev. Lett.* **77**, 2518 (1996).
 - [9] B. S. Stipe, M. A. Rezaei, and W. Ho, *J. Chem. Phys.* **107**, 6443 (1997).
 - [10] D. Arvanitis, U. Dobler, L. Wenzel, K. Baberschke, and J. Stöhr, *Surf. Sci.* **178**, 686 (1986).
 - [11] X. F. Hu, C. J. Chen, and J. C. Tang, *Surf. Sci.* **365**, 319 (1996).
 - [12] G. P. Salam, M. Persson, and R. E. Palmer, *Phys. Rev. B* **49**, 10 655 (1994).
 - [13] B. S. Stipe, M. A. Rezaei, and W. Ho, *Science* **280**, 1732 (1998).
 - [14] M. A. Gata and P. R. Antoniewicz, *Phys. Rev. B* **47**, 13 797 (1993).
 - [15] A. Laubereau and W. Kaiser, *Rev. Mod. Phys.* **50**, 607 (1978).
 - [16] F. Legay, in *Chemical and Biological Applications of Lasers*, edited by C. B. Moore (Academic, New York, 1977), p. 43.
 - [17] K. F. Freed and H. Metiu, *Chem. Phys. Lett.* **48**, 262 (1977).
 - [18] H. Dubost, *Chem. Phys.* **12**, 139 (1976).
 - [19] A. L. Harris, L. Rothberg, L. H. Dubois, N. J. Levinos, and L. Dhar, *Phys. Rev. Lett.* **64**, 2086 (1990).
 - [20] P. Guyot-Sionnest, P. Dumas, Y. J. Chabal, and G. S. Higashi, *Phys. Rev. Lett.* **64**, 2156 (1990).
 - [21] Ts. S. Marinova and P. K. Stefanov, *Surf. Sci.* **191**, 66 (1987).